Electronic Supplementary Material (ESI) for Journal of Materials Chemistry A.
This journal is © The Royal Society of Chemistry 2021

Supplementary Information

One Dimensional Graphene Nanoscroll-Wrapped MnO Nanoparticles for High-Performance Lithium Ion Hybrid Capacitors

Bingjun Yang,[ac] Jiangtao Chen,[a] Bao Liu,[ac] Yunxia Ding,[a] Yu Tang,[b]* and Xingbin Yan[acd]*

[a]Laboratory of Clean Energy Chemistry and Materials, State Key Laboratory of Solid Lubrication, Lanzhou Institute of Chemical Physics, Chinese Academy of Sciences, Lanzhou 730000, China

[b]State Key Laboratory of Applied Organic Chemistry, Key Laboratory of Nonferrous Metal Chemistry and Resources Utilization of Gansu Province, College of Chemistry and Chemical Engineering, Lanzhou University, Lanzhou 730000, China

[c]Center of Materials Science and Optoelectronics Engineering, University of Chinese Academy of Sciences, Beijing 100049, China

[d]Dalian National Laboratory for Clean Energy, Dalian 116023, China

*Corresponding authors Xingbin Yan, Yu Tang

E-mail: xbyan@licp.cas.cn, tangyu@lzu.edu.cn

Keywords: graphene nanoscroll, MnO, anode, 3D framework activated carbon, lithium-ion hybrid capacitors.

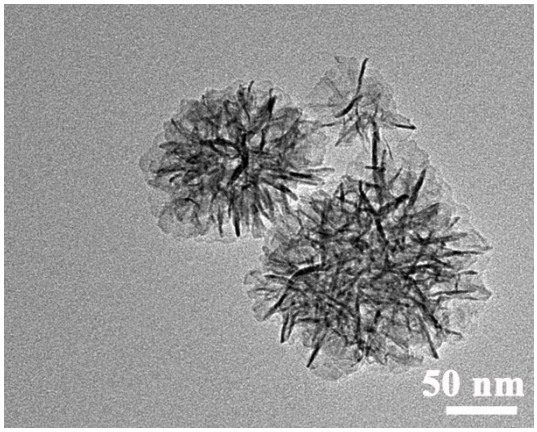

Figure S1. High magnification TEM image of spherical K_xMnO_2 precursors.

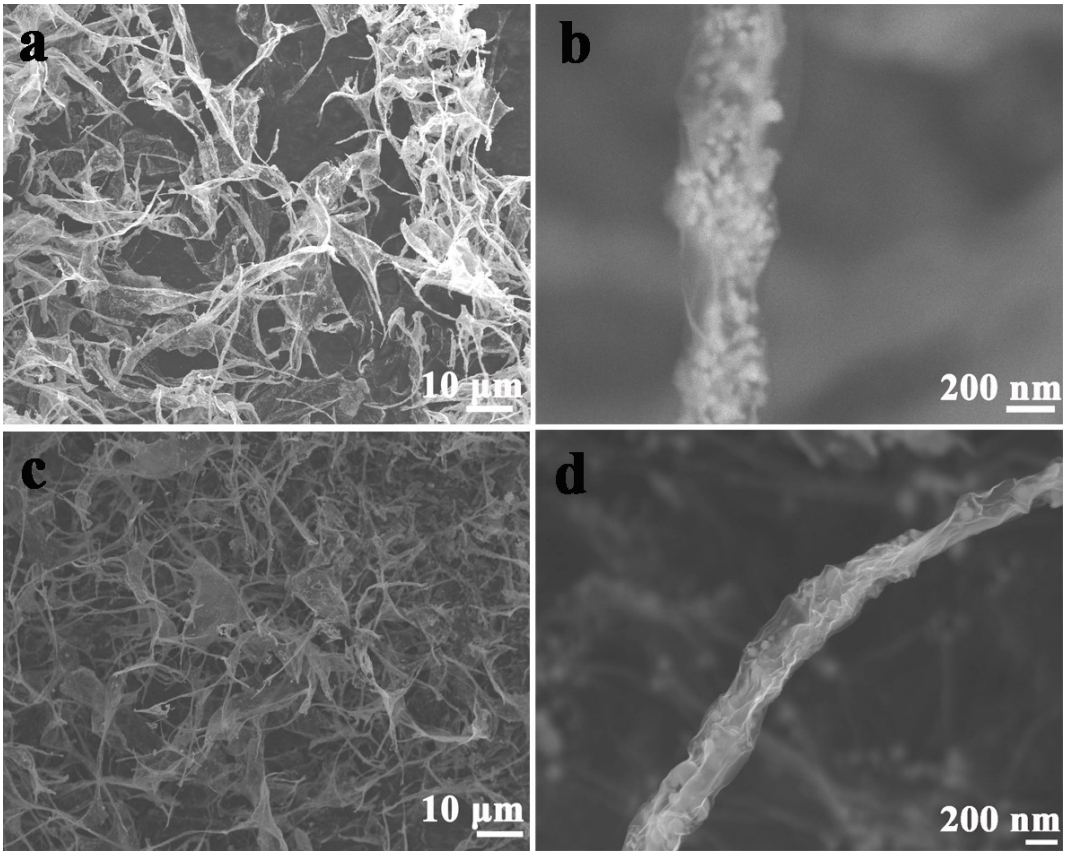

Figure S2. High and low magnification SEM images of GNS@MnO with different Calcination temperature: (a,b) GNS@MnO_x-400, (c,d) GNS@MnO-800.

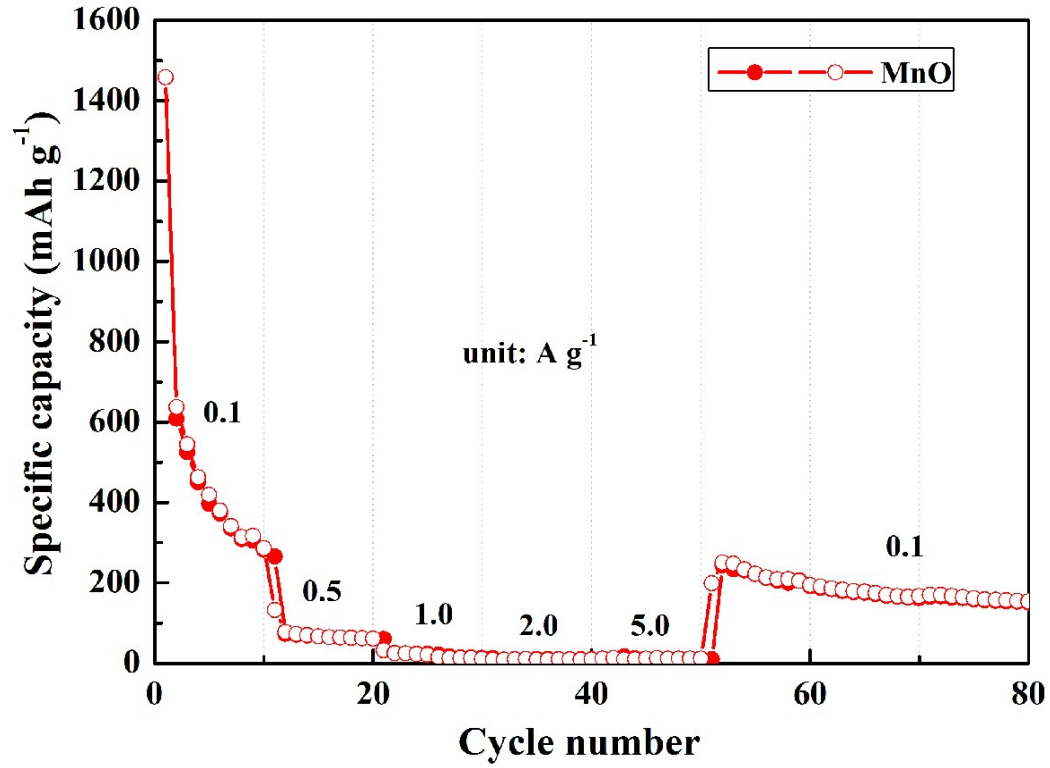

Figure S3. Rate performance of pure MnO electrode.

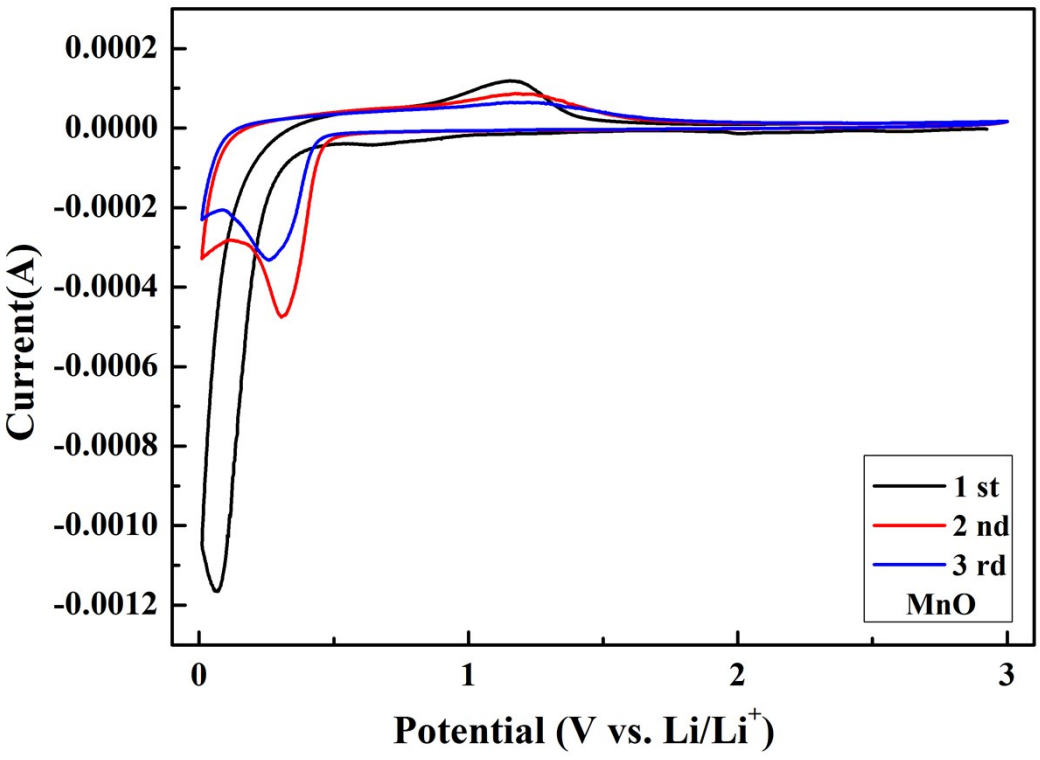

Figure S4. The first three CV curves of MnO at a scan rate of 0.1 mV s^{-1}.

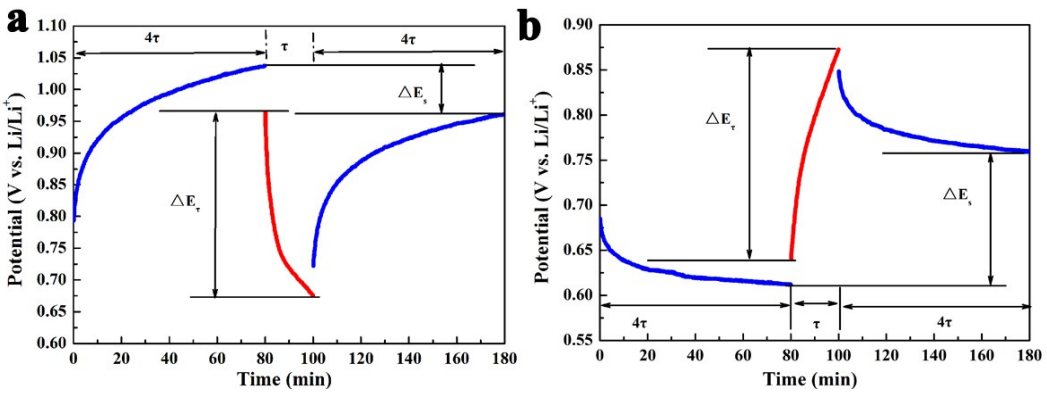

Figure S5. Scheme for voltage response with time during a single constant current pulse: (a) Discharge. (b) Charge.

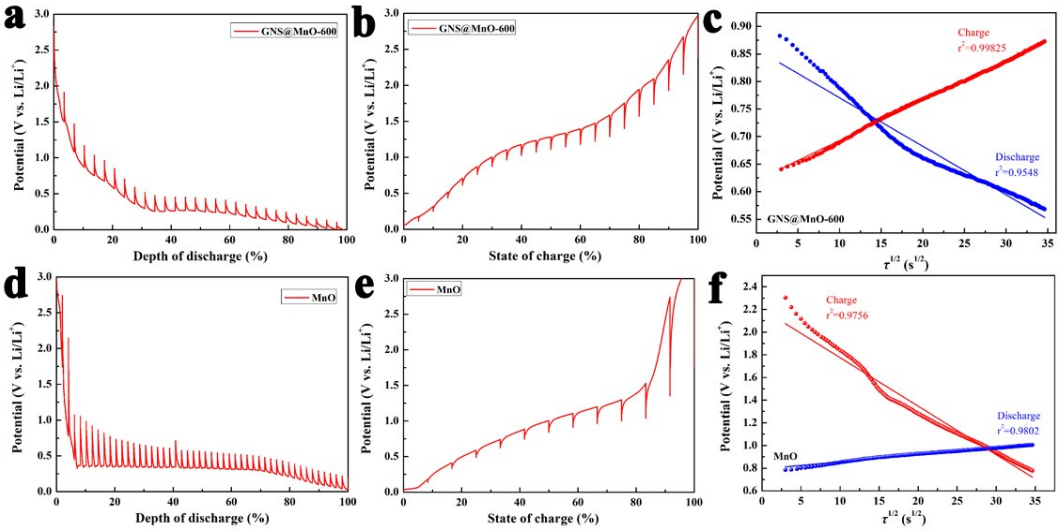

Figure S6.GITT characterization: GITT potential profiles of (a) discharge and (b) charge for GNS@MnO-600 anode. (c) Variation of cell potential during single charge and discharge titration plotted against$\tau^{1/2}$ for GNS@MnO-600 anode. GITT potential profiles of (d) discharge and (e) charge for MnO anode. (f) Variation of cell potential during single charge and discharge titration plotted against $\tau^{1/2}$ for pure MnO anode.

GITT is an effective strategy to estimate the apparent Li^+ ion diffusion coefficient at different quasi-equilibrium potentials. During the test, a relatively small titration current density (i.e., 0.1 A g^{-1}) is applied for a relatively short period (i.e., τ = 20 min

= 1200 s) to induce a potential shift (ΔEτ), followed by much longer relaxation period (i.e., 4τ = 80 min = 4800 s) to reach a quasi-equilibrium potential for the calculation of ΔEs (Figure S5). The above titration-relaxation cycle is performed continuously at the whole potential window (i.e., 0.01-3.0 V vs. Li/Li^+) to give a completed potential profile (Figure S6).

The apparent Li^+ diffusion coefficient (D, $cm^2\ s^{-1}$) is calculated based on Fick's second law of diffusion (equation S1):[1, 2]

$$D = \frac{4}{\pi}\left(\frac{mV_m}{MA}\right)^2\left(\frac{\Delta E_s/\tau}{dE_\tau/d\sqrt{\tau}}\right)^2 \quad \text{(S1)}$$

where m(g) is mass loading, Vm ($cm^3\ mol^{-1}$) is molar volume of the electrode, M (g mol^{-1}) is molar weight of the electrode, A (cm^2) is electroactive area of the electrode, ΔEs (V) is the change of quasi-equilibrium potential after two sequential relaxation period, τ (s) is charge or discharge time during each titration, $dE_\tau/d\sqrt{\tau}$ ($V\ s^{-1/2}$) is potential shift rate.

The above equation S1 can be simplified as equation S2 by applying the small current density for a sufficiently short time in each titration.

$$D = \frac{4}{\pi\tau}\left(\frac{mV_m}{MA}\right)^2\left(\frac{\Delta E_s}{\Delta E_\tau}\right)^2 \quad \text{(S2)}$$

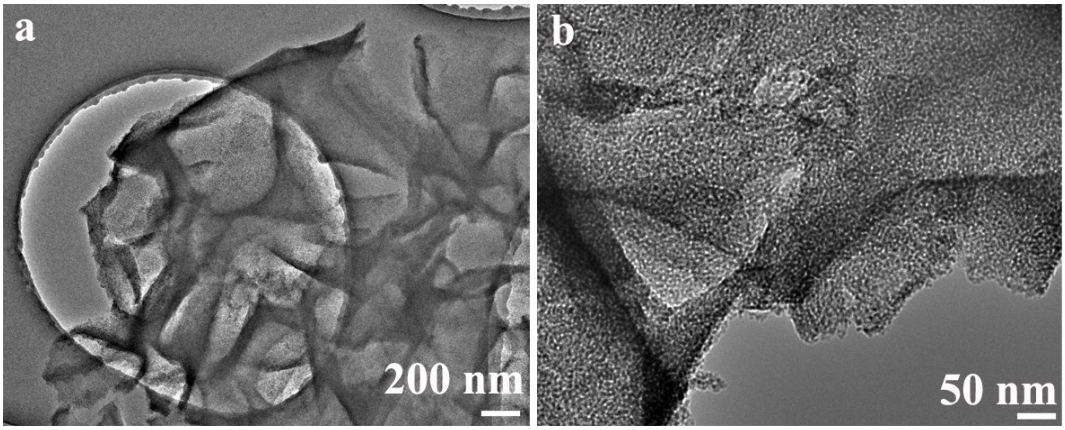

Figure S7.TEM images of 3DFAC

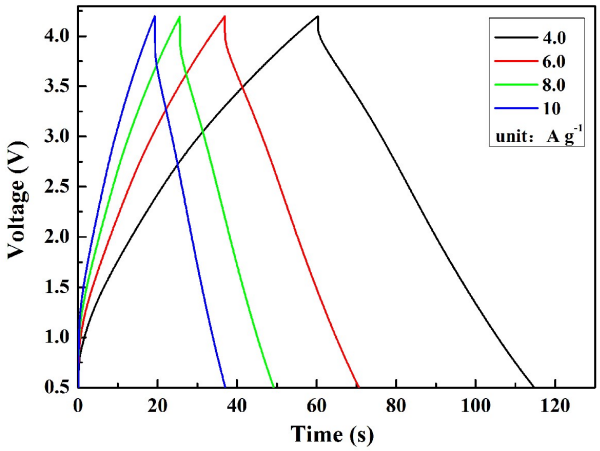

Figure S8. GCD profiles of GNS@MnO-600//3DFAC LIHC (1:1) at high current density.

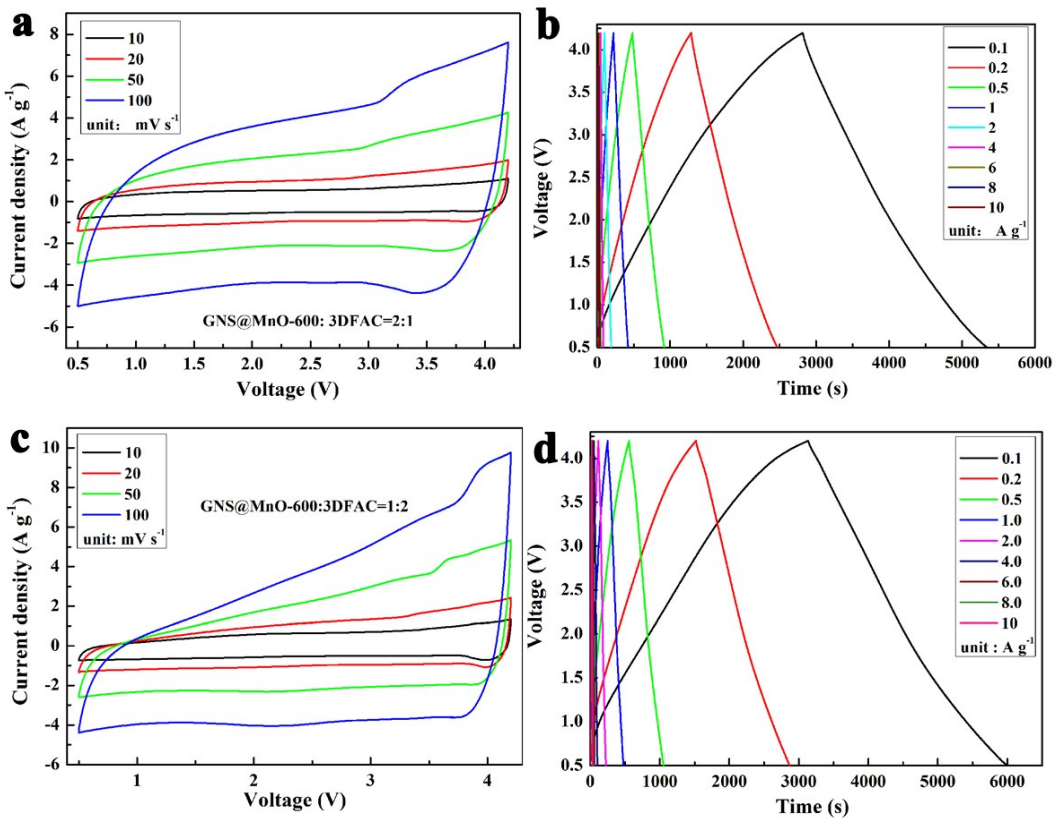

Figure S9. CVs and GCD profiles of GNS@MnO-600//3DFAC LIHCs with different mass ratios: (a, b) 2:1; (c, d) 1:2.

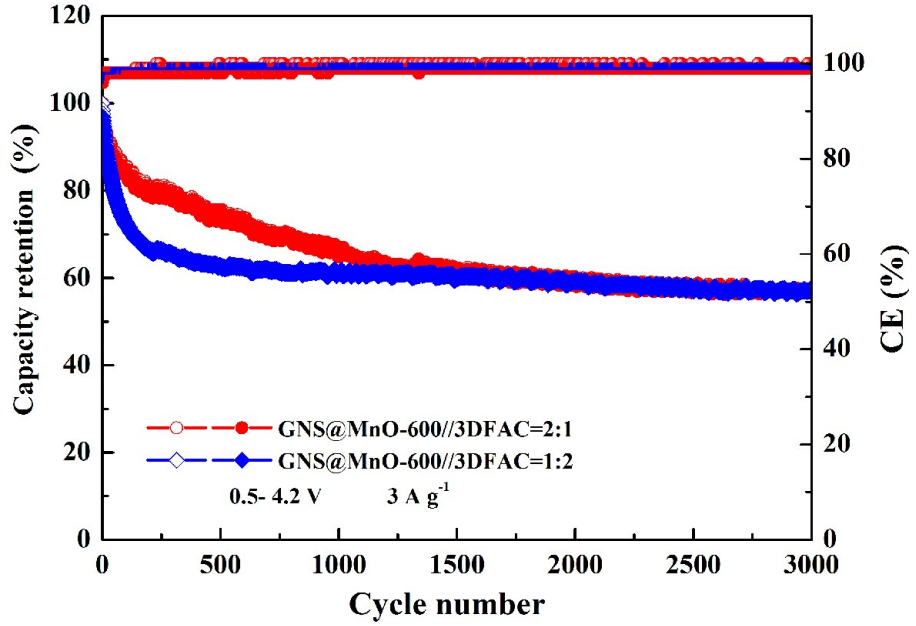

Figure S10. Cycling stability of the as-assembled GNS@MnO-600//3DFAC devices with mass ratios of 2:1 and 1:2.

Table S1. Comparison of the electrochemical performances of the as-prepared 1D GNS@MnO-600 anode with other MnO-C anode materials for LIBs reported previously.

Materials	Rate performance	Ref.
MnO@NC/ graphite	0.1 A g^{-1} / 835 mA h g^{-1} 5.0 A g^{-1} / 387 mA h g^{-1}	3
NC/MnO/RGO	0.1 A g^{-1} / 925.9 mA h g^{-1} 5.0 A g^{-1} / 355.5 mA h g^{-1}	4
MnO@HCF-2	0.1 A g^{-1} / 586.8 mA h g^{-1} 4.0 A g^{-1} / 327.8 mA h g^{-1}	5
MnO@N-CS	0.2 A g^{-1} / 917mA h g^{-1} 5.0 A g^{-1} / 328 mA h g^{-1}	6
MnO/Mn3O4/N-graphene	0.5 A g^{-1} / 681 mA h g^{-1} 2.0 A g^{-1} / 365 mA h g^{-1}	7
MnO/N-PCNTs	0.1 A g^{-1} / 652 mA h g^{-1} 1.0 A g^{-1} / 220 mA h g^{-1}	8
MnO/Metal/Carbon	0.1 C / 600 mA h g^{-1} 5.0 C / 200 mA h g^{-1}	9
Sn-MnO@CYINs	0.2 A g^{-1} / 662 mA h g^{-1} 2.0 A g^{-1} / 402 mA h g^{-1}	10
RGO-MnO@NC	0.5 A g^{-1} / 599 mA h g^{-1} 5.0 A g^{-1} / 331 mA h g^{-1}	11
C/MnO/SiOC	0.1 A g^{-1} / 684 mA h g^{-1} 2.0 A g^{-1} / 408 mA h g^{-1}	12
MnO-PS	0.1 A g^{-1} / 960 mA h g^{-1} 2.0 A g^{-1} / 300 mA h g^{-1}	13
1D GNS@MnO-600	**0.1 A g^{-1}/ 766 mA h g^{-1}** **5.0 A g^{-1} / 437 mA h g^{-1}**	**This work**

References

1 W. Weppner and R. A. Huggins, *J. Electrochem. Soc.*, 1977, **124**, 1569-1578.

2 H. Li, J. Chen, L. Zhang, K. Wang, X. Zhang, B. Yang, L. Liu, W. Liu and X. Yan, *J. Mater. Chem. A*, 2020, **8**, 16302-16311.

3 Y. Xue, H. Li, M. Zhang, W. Yu, K. Zhuo and G. Bai, *J. Alloys Compd.*, 2020, **848**, 156571.

4 G. Li, Z. Li, Z. Hou, Y. Liu and S. Jiao, *Electrochim. Acta*, 2020, **363**, 137184.

5 Z.-Y. Chen, B. He, D. Yan, X.-F. Yu and W.-C. Li, *J. Power Sources*, 2020, **472**, 228501.

6 S. Huang, H. Li, G. Xu, X. Liu, Q. Zhang, L. Yang, J. Cao and X. Wei, *Electrochim. Acta*, 2020, **342**, 136115.

7 C. Zhou, K. Zhang, M. Hong, Y. Yang, N. Hu, Y. Su, L. Zhang and Y. Zhang, *Chemical Engineering Journal*, 2020, **385**, 123720.

8 P. Mu, W. Ma, Y. Zhao, C. Zhang, S. Ren, F. Wang, C. Yan, Y. Chen, J. H. Zeng and J.-X. Jiang, *J. Power Sources*, 2019, **426**, 33-39.

9 X. Wang, L. Ma, Q. Ji, J.-Q. Meng, S. Liang, Z. Xu, M. Wang, X. Zuo, Y. Xiao, J. Zhu, Y. Xia, P. Müller-Buschbaum and Y.-J. Cheng, *Adv. Mater. Interfaces*, 2019, **6**, 1900335.

10 F. Zhang, Y. Wang, W. Guo, S. Rao and P. Mao, *Chemical Engineering Journal*, 2019, **360**, 1509-1516.

11 Y. Wang, H. Wu, Z. Liu, H. Zhao, H. Liu and Y. Zhang, *Inorg. Chem.*, 2018, **57**, 13693-13701.

12 H. Huang, C. Shi, R. Fang, Y. Xia, C. Liang, Y. Gan, J. Zhang, X. Tao and W. Zhang, *Chemical Engineering Journal*, 2019, **359**, 584-593.

13 P. Remith and N. Kalaiselvi, *Phys. Chem. Chem. Phys.*, 2016, **18**, 15854-15860.